

行政院國家科學委員會補助專題研究計畫  成果報告  
 期中進度報告

(計畫名稱)

速度—渦度之不可壓縮黏性流分析(II)

計畫類別： 個別型計畫  整合型計畫

計畫編號：NSC 90 - <sup>611</sup>2811 - E - 002 - <sup>024</sup>008

執行期間：90年8月1日至91年7月31日

計畫主持人：許文翰教授

共同主持人：

計畫參與人員：

成果報告類型(依經費核定清單規定繳交)： 精簡報告  完整報告

本成果報告包括以下應繳交之附件：

- 赴國外出差或研習心得報告一份
- 赴大陸地區出差或研習心得報告一份
- 出席國際學術會議心得報告及發表之論文各一份
- 國際合作研究計畫國外研究報告書一份

處理方式：除產學合作研究計畫、提升產業技術及人才培育研究計畫、  
列管計畫及下列情形者外，得立即公開查詢

涉及專利或其他智慧財產權， 一年  二年後可公開查詢

執行單位：國立台灣大學工程科學及海洋工程學系所

中華民國九十二年四月十五日

## 中文摘要

本文係以速度—渦度為主要變數求解穩態不可壓縮黏性流之 Navier-Stokes 方程式。方法以求解包含速度之二階微分方程式及渦度之 convection-diffusion 方程式，並建立其適當之渦度邊界條件。對於本文中所精巧設計建立之渦度積分邊界條件，將透過程式之驗證以確定立數值求解之優越性。

**關鍵詞：**有限差分方法、不可壓縮、Navier-Stokes、速度—渦度

## **Abstract**

We consider in this progress report for solving the steady-state Navier-Stokes equations for incompressible fluid flows using velocities and vorticity as working variables. The method involves solving a second-order differential equation for the velocity and a convection-diffusion equation for the vorticity. The key to the success of the numerical simulation of this class of flow equations depends largely on proper simulation of vorticity transport equation subject to proper vorticity boundary condition. While the derivation of the proposed integral vorticity boundary condition is more elaborate and is more difficult to solve than conventional local approaches, we will demonstrate its significant advantages by virtue of benchmark tests.

**Keywords:** finite difference, incompressible, Navier-Stokes, velocity-vorticity

# 目錄

中文摘要.....	1
英文摘要.....	錯誤! 尚未定義書籤。
目錄.....	3
1. Introduction.....	4
2. Mathematical model.....	5
3. Vorticity integral condition.....	6
4. Numerical results .....	7
4.1 Lid-driven cavity flow problem.....	7
4.2 Backward-facing step problem.....	8
5. Concluding remarks .....	9
Reference.....	10
Figures.....	11
誌謝.....	13

# 1. Introduction

The traditional approach to the numerical solution for incompressible Navier-Stokes equations has been to solve working equations in velocity-pressure variables. A serious problem which was encountered while performing the primitive variable formulation is owing to the absence of pressure in the continuity equation. In addition, discretization of pressure gradients in the incompressible equations on curvilinear grids presents considerable difficulties owing to the fact that the approximation of pressure gradient operator should be irrotational [1]. While this difficulty can be effectively resolved on staggered grids [2], special care is needed when grids are non-uniformly and non-orthogonally laid on the flow [1]. It is the added grid complexity that complicates further the incompressible flow analysis. Another popular approach to numerical solution of the Navier-Stokes equations is the velocity-vorticity approach. This formulation is the most appropriate choice for solving the vortex dominated flow. The reason lies in the fact that the advection of vorticity is the most important process determining the flow dynamics. Additionally, it appears that studying incompressible Navier-Stokes equations in terms of vorticity and velocity is closer to physical reality [3]. For the present spatial discretization on collocated grids, we abandon the DC problem and confine ourselves to the second-order Poisson equations to solve for velocity components. Another second-order differential equation for the vorticity scalar must be solved subject to proper boundary conditions, which are the subject of the present study. An accurate prediction of the transport of vorticity is another consideration. We will address this issue in the use of an exponential compact scheme for the flux discretization.

## 2. Mathematical model

The traditional approach to the numerical solution of incompressible Navier-Stokes equations has been the primitive-variable formulation. Using the kinematic definition of the vorticity  $\underline{\omega} = \nabla \times \underline{u}$ , the resulting transport equation is derived as

$$\underline{u} \cdot \nabla \underline{\omega} - \underline{\omega} \cdot \nabla \underline{u} = \frac{1}{\text{Re}} \nabla^2 \underline{\omega} \quad (1)$$

The vorticity stretching term,  $\underline{\omega} \cdot \nabla \underline{u}$ , represents the generation or destruction of vorticity due to the stretching or compression of the vortex line. As the space dimension decreases by one, the vortex stretching term vanishes in two-dimensional cases, and the resulting vorticity transport equation is reduced to a scalar equation for the vorticity component which is normal to the planar motion of the flow :

$$\underline{u} \cdot \nabla \underline{\omega} = \frac{1}{\text{Re}} \nabla^2 \underline{\omega} \quad (2)$$

The working equations for the velocity components can also be obtained by taking the curl of the definition  $\underline{\omega} = \nabla \times \underline{u}$  and by using the continuity equation. The resulting second-order Poisson equations for velocity components  $u$  and  $v$  are derived, respectively, as

$$\begin{aligned} \nabla^2 u &= -\omega_y \\ \nabla^2 v &= \omega_x \end{aligned} \quad (3)$$

The theoretical equivalence between this classical second-order velocity-vorticity formulation and the velocity-pressure formulation has been given. For the details we refer to the paper by Daube et al. [4].

### 3. Vorticity integral condition

The key element in the vorticity-velocity formulation is to obtain the a priori unknown boundary values of the vorticity for the second-order transport equation (1). The theory behind our derivation of the vorticity boundary condition is the Green's identity, which relates two scalar potentials and as follows:

$$\int_{\Omega} \phi \nabla^2 \psi - \psi \nabla^2 \phi \, dA = \oint (\phi \frac{\partial \psi}{\partial n} - \psi \frac{\partial \phi}{\partial n}) \, ds \quad (4)$$

Provided that the scalar potential is assigned as the stream function, the following two equations ensure satisfaction of mass conservation :

$$\begin{aligned} u &= \frac{\partial \psi}{\partial y} \\ v &= -\frac{\partial \psi}{\partial x} \end{aligned} \quad (5)$$

Now, let be the scalar potential which satisfies the Laplace equation. The boundary value of is enforced to be zero everywhere except at one point where the value is one :

$$\begin{aligned} \nabla^2 \phi &= 0 \quad \text{in } \Omega \\ \phi_i &= \delta_{ij} \quad \text{on } \Omega \end{aligned} \quad (6)$$

We can get

$$\int_{\Omega} \phi \omega \, dA = \oint_{\partial \Omega} \phi u_{\tau} \, ds + \int_{\Omega} (v \frac{\partial \phi}{\partial x} - u \frac{\partial \phi}{\partial y}) \, dA$$

where  $u_{\tau} = -\frac{\partial \psi}{\partial n} |_{\partial \Omega}$ .

This completes the derivation of the vorticity integral equation for the transport equation (1). It is worth noting that the assignment of =1 leads to

$$\int_{\Omega} \omega \, dA = \oint_{\partial \Omega} u_{\tau} \, ds$$

## 4. Numerical results

### 4.1 Lid-driven cavity flow problem

We present a two-dimensional simulation for the fluid flow in a square cavity defined by  $B:D=1:1$ . The Reynolds numbers chosen for this study was 1000, which were computed based on the lid speed, the width of the cavity, and the kinematic viscosity of the fluid. In this study, the solutions were computed on uniform grids of  $131 \times 131$  for  $Re=1000$ . For comparison purposes, the velocity profiles of Ghia et al. [5] are also plotted in Fig. 1.



## 4.2 Backward-facing step problem

Expansion flows in straight channels with have been another focus of intensive study over the last few decades and have been the subject of an international workshop [7]. Although this flow represents one of the simplest expansion flows, the physics involved are rather complex due to the formation of recirculating vortices and flow reversals downstream of the step. We consider this problem to be computationally important because of the availability of experimental data [5, 6] and the simplicity of the geometry.

Several Reynolds numbers,  $Re=100, 200, 400, 500$  and  $800$ , were considered in this study. Among the basic features pertinent to the problem, as illustrated in Fig. 2, is the flow separation from the step corner. As in many real flows, separation of a boundary layer is followed by downstream reattachment to a solid wall. Determining the reattachment location, as measured from the step, is, thus, the primary focus of this study. It is also important to see the separation-reattachment eddy on the channel roof.

Notwithstanding, the importance of eddy formation in the channel, we plot reattachment lengths of the primary eddy behind the step in Fig. 3 for cases with different Reynolds numbers. We compared our results with measurement data [8] as well as other numerical data [9, 10] for the sake of completeness. We also plot the separation length of the roof eddy in Fig. 14 and compare results with experimental [8] and numerical [9] data for the Reynolds numbers considered in this study. Fig. 4 plots the reattachment location of the roof eddy together with data given by Armaly et al. [8] and Gartling [9]. From this comparison, it is now considered that our compact scheme is applicable to Navier-Stokes flow simulations of the vertical flow structure.

## 5. Concluding remarks

The goal for the present study was to simulate incompressible viscous flows by means of the velocity-vorticity formulation. In order for the solutions to be accurately predicted, it is important to develop a theoretically rigorous framework which can provide us with boundary vorticity without using field variables outside of the physical domain. The equation governing the boundary vorticity is derived in integral form. Thus, boundary vorticities are simultaneously solved from the matrix equation. The solution algorithm involves a scalar transport equation for the vorticity variable and two Poisson equations for velocity components. Specific to our flux discretization scheme is that the coefficient matrix of the compact nine-point stencil scheme is classified as an irreducibly diagonal dominant M-matrix. To better understand the compact finite difference scheme developed here, we have conducted computational exercises. In the Navier-Stokes flow analyses, we have considered the lid-driven cavity and backward-facing step problems. The results demonstrate that the integral approach designed to provide the boundary vorticity is applicable to simulation of fluid flows which are vortical in nature.

## Reference

- [1] R. S. Bernard, Hartmut Kapitza, How to discretize the pressure gradient for curvilinear MAC grids, *J. Comput. Phys.* 99 (1992) 288-298.
- [2] E. Wienan and Jian-Guo Liu, Finite difference methods for 3D viscous incompressible flows in the vorticity-vector potential formulation on nonstaggered grids, *J. Comput. Phys.* 138 (1997) 57-82.
- [3] H. J. H. Clercx, A spectral solver for the Navier-Stokes equations in the velocity-vorticity formulation for flows with two nonperiodic directions, *J. Comput. Phys.* 137 (1997) 186-211.
- [4] O. Daube, J. C. Guermond and A. Sellier, Sur la formulation vitesse-toubillon des equations de Navier-Stokes en ecoulement incompressible, *C. R. Acad. Sci, Paris*, 313, serie II (1991) 377-382.
- [5] U. Ghia, K. N. Ghia, and C. T. Shin, High-Re solutions for incompressible flow using the Navier-Stokes equations and a multigrid method, *J. Comput. Phys.* 48 (1982) 387-411.
- [6] M. Deville, T. H. Lê, Y. Morchoisneceds, Numerical Simulation of 3D Incompressible ?Unsteady Viscous Laminar Flows, 36, NNFPM, 1992.
- [7] K. Morgan, J. Periaux, F. Thomasset (Eds.), Analysis of Laminar Flow over a Backward-Facing Step, A GAMM-Workshop, Friedr Viewly and Sohn, Germany, 1984.
- [8] B. F. Armaly, F. Durst, J. C. F. Pereira, B. Schönung, Experimental and theoretical investigation of backward-facing step flow, *J. Fluid Mech.* 127 (1983) 473-496.
- [9] D. K. Gartling, A test problem for outflow boundary condition — Flow over a backward-facing step, *Int. J. Numer. Fluid*, 11(1990) 953-967.
- [10] G. A. Osswald, K. N. Ghia, U. Ghia, Study of incompressible separated flow using an implicit time-dependent technique, in: AIAA, Sixth CFD Conference, vol. 686, Denver, MA, 1983.

# Figures

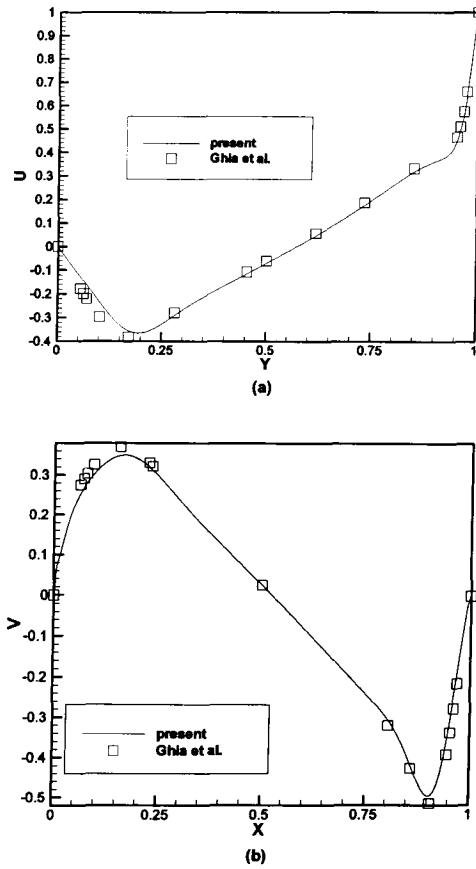


Fig. 1: Velocity profiles plotted on the centerlines for the case  $Re=1000$  (a)  $u$ - $y$  plot at  $x=0.5$ ; (b)  $v$ - $x$  plot at  $y=0.5$ .

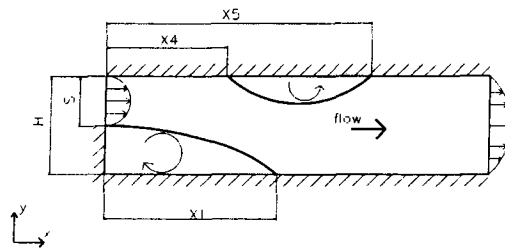


Fig. 2: Schematic of the backward-facing step problem considered in Section 4.2.

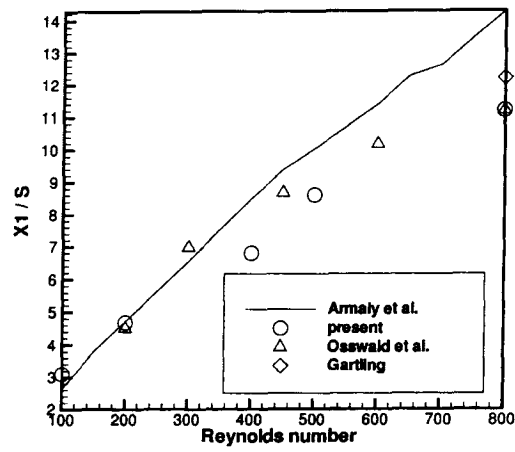


Fig. 3: The reattachment locations,  $x_1$  on the floor of the channel versus  $Re$ .

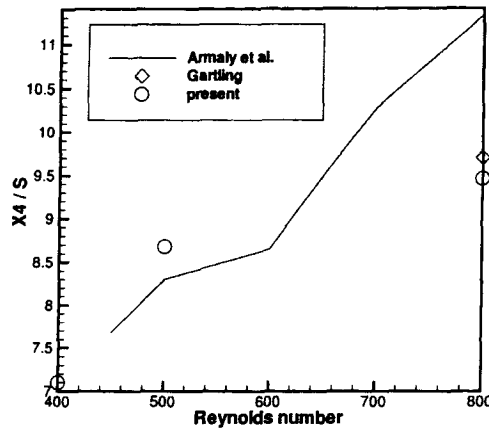


Fig. 4: The separation locations,  $x_4$  on the roof of the channel against  $Re$ .

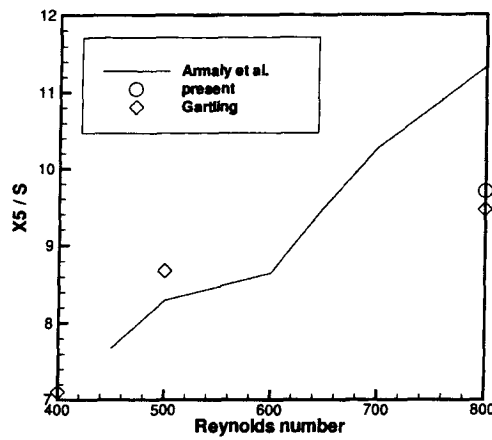


Fig. 5: The reattachment locations,  $x_5$  on the floor of the channel against  $Re$ .

## 誌謝

本計劃承國家高速電腦中心及計劃NSC 90-2811-E-002-008之經費補助，而得以進行，在此特予誌謝。